IOPscience iopscience.iop.org

Home Search Collections Journals About Contact us My IOPscience

Excitation of global eigenmodes of the Alfven wave in Tokamaks

This content has been downloaded from IOPscience. Please scroll down to see the full text.

1982 Plasma Phys. 24 1147

(http://iopscience.iop.org/0032-1028/24/9/010)

View the table of contents for this issue, or go to the journal homepage for more

Download details:

IP Address: 134.151.40.2
This content was downloaded on 20/01/2014 at 07:18

Please note that terms and conditions apply.

Plasma Physics, Vol. 24, No. 9, pp. 1147 to 1159, 1982
Printed in Great Britain.

0032-1028/82/091147-13$03.00/0
© 1982 Institute of Physics and Pergamon Press Ltd.

EXCITATION OF GLOBAL EIGENMODES OF THE ALFVEN WAVE IN TOKAMAKS

K. APPERT, R. GRUBER, F. TROYON and J. VACLAVIK
Centre de Recherches en Physique des Plasmas, Association Euratom-Confédération Suisse,
Ecole Polytechnique Fédérale de Lausanne, CH-1007 Lausanne, Switzerland

(*Received* 6 *January* 1982; *and in revised form* 17 *March* 1982)

Abstract—Analytical and numerical results which demonstrate the existence of a new class of eigenmodes of the Alfvén wave are presented. Possible implications for low frequency heating of Tokamaks are discussed.

1. INTRODUCTION

RECENT experimental (DE CHAMBRIER *et al.*, 1981) and numerical (ROSS *et al.*, 1981) results concerning the antenna loading for Alfvén wave heating of Tokamak plasmas show evidence of resonance peaks at frequencies just below the lower edge of the Alfvén continuum. A similar peak has been noticed in the calculations of MHD spectra by POCHELON *et al.* (1975). The objective of this paper is to provide a simple interpretation of this phenomenon by means of the ideal MHD theory. In particular, we shall show that the resonance peaks can be related to the excitation of a new class of eigenmodes of the Alfvén wave. We propose to call these modes "global eigenmodes" to distinguish them from the well-known singular eigenmodes. We also discuss the possibility of using these modes for an "Alfvén Eigenmode Resonance Heating" (AERH) scheme of Tokamak plasmas.

The plan of the paper is as follows. In Section 2 we present the basic equations of the ideal MHD model for a low-β plasma in cylindrical geometry, together with a short discussion of the continuous spectrum. In Section 3 we demonstrate the existence of the global eigenmodes of the Alfvén wave by means of a WKB approach and through numerical calculations performed using the one-dimensional spectral code THALIA (APPERT *et al.*, 1975). In Section 4 we present analytical calculations which predict that, in some circumstances, the lower edge of the Alfvén continuum is an accumulation point of the global eigenmodes. Section 5 deals with the effects of toroidicity. Finally, in Section 6 we put forward some ideas about using these modes for low frequency heating of Tokamaks.

2. BASIC EQUATIONS AND CONTINUOUS SPECTRUM

A circular cross-section Tokamak with a large aspect ratio R/a can be considered as a straight cylindrical plasma column with the usual correspondence, $k = n/R$, between the longitudinal (z-direction) wavenumber k and the toroidal wavenumber n. (R and a are the major and minor radii, respectively.) Denoting by m the azimuthal (θ-direction) wavenumber, the linear displacement vector $\boldsymbol{\xi} = (\xi_r, \xi_\theta, \xi_z)$ can be Fourier-analysed in time, θ and z:

$$\boldsymbol{\xi}(t, r, \theta, z) = \boldsymbol{\xi}(r) \exp[i(\omega t + m\theta + kz)], \tag{1}$$

where r is the remaining independent radial variable. In the ideal MHD model, an eigenfrequency ω and the corresponding eigenfunction $\xi(r)$ can be obtained by solving the Hain–Lüst equation (HAIN and LÜST, 1958) with appropriate boundary conditions. For a low-β plasma, the terms proportional to the adiabaticity index γ may be neglected and the equation reduces to

$$\frac{\mathrm{d}}{\mathrm{d}r}\left[\frac{AB^2}{N}\frac{1}{r}\frac{\mathrm{d}}{\mathrm{d}r}(r\xi_r)\right]+\left[\mu_0 A - r\frac{\mathrm{d}}{\mathrm{d}r}\left(\frac{B_\theta}{r}\right)^2 - \frac{4k^2B_\theta^2B^2}{\mu_0 r^2 N}+\frac{r}{\mu_0}\frac{\mathrm{d}}{\mathrm{d}r}\left(\frac{2kB_\theta GB^2}{r^2N}\right)\right]\xi_r = 0, \tag{2}$$

where

$$A = \rho\omega^2 - \frac{F^2}{\mu_0}, \quad N = A - \frac{G^2}{\mu_0},$$

$$F = \mathbf{k}\cdot\mathbf{B} \equiv kB_z + \frac{m}{r}B_\theta,$$

$$G = \mathbf{k}\times\mathbf{B} \equiv \frac{m}{r}B_z - kB_\theta.$$

The quantities $\mathbf{B} = (0, B_\theta, B_z)$ and ρ are the equilibrium magnetic field and mass density, respectively. The plasma is surrounded by a vacuum region which is limited by a concentric wall.

For a given k and m, equation (2) possesses one continuous spectrum (APPERT *et al.*, 1974) defined by $A = 0$, the so-called Alfvén continuum. Its range is given by

$$\mathrm{Min}[\omega_A^2(r)] \leqslant \omega^2 \leqslant \mathrm{Max}[\omega_A^2(r)], \tag{3}$$

where

$$\omega_A^2 = \frac{F^2}{\rho\mu_0}. \tag{4}$$

It is well known that besides this continuum, equation (2) possesses different discrete spectra. In particular, all unstable modes are associated with a discrete spectrum. The eigenmodes of the fast magnetoacoustic wave are associated with a discrete spectrum which has an accumulation point at $\omega = \infty$.

An example of the dependence on n of the Alfvén continuum is shown in Fig. 1. The curves corresponding to the Alfvén frequencies at the axis ($\omega_A^2(0)$) and the plasma surface ($\omega_A^2(a)$) are drawn as solid lines. The dotted line represents the lower edge of the Alfvén continuum corresponding to the local Alfvén frequency somewhere inside the plasma. At this radial position we have

$$\frac{\mathrm{d}\omega_A^2}{\mathrm{d}r} = 0, \tag{5}$$

while at $r = 0$ and $n = n_c$

$$\frac{\mathrm{d}\omega_A^2}{\mathrm{d}r} = \frac{\mathrm{d}^2\omega_A^2}{\mathrm{d}r^2} = \frac{\mathrm{d}^3\omega_A^2}{\mathrm{d}r^3} = 0. \tag{6}$$

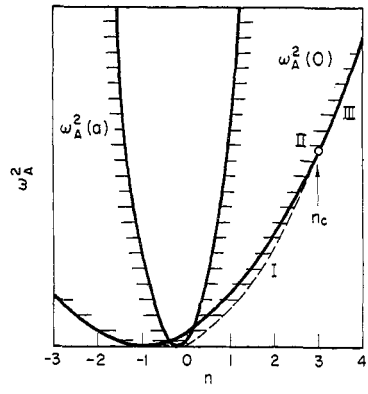

FIG. 1.—Continuous spectrum (hatched region) vs n for fixed m. The curves $\omega_A^2(0)$ and $\omega_A^2(a)$ represent the Alfvén frequencies at the axis and at the plasma surface, respectively. The dashed curve is the lower edge of the continuum corresponding to a local Alfvén frequency somewhere inside the plasma (region I). At $n = n_c$ (II), an essential singularity appears at the plasma axis. In region III the lower edge of the Alfvén continuum is determined by $\omega_A^2(0)$.

3. GLOBAL EIGENMODES OF THE ALFVEN WAVE

The recent experimental results obtained on the TCA Tokamak at Lausanne (DE CHAMBRIER *et al.*, 1981) and the numerical results obtained by ROSS *et al.* (1981) suggest the existence of one or more weakly-damped eigenmodes at frequencies just below the lower edge of the Alfvén continuum. At first glance, this is a surprising finding. However, a simple inspection of equation (2) may already shed some light on the phenomenon. Indeed, on performing a WKB-type of analysis of this equation one finds a new class of eigenmodes whose dispersion relation reads

$$\omega^2 = \omega_A^2 - \frac{1}{k_r^2 \rho \mu_0}\left[\left(\frac{2B_\theta}{r}\right)^2 k^2 + \left(\frac{G}{B}\right)^2 r \frac{\mathrm{d}}{\mathrm{d}r}\left(\frac{B_\theta}{r}\right)^2\right], \tag{7}$$

where k_r is the radial wavenumber.

These modes can be found numerically by means of the one-dimensional spectral code THALIA (APPERT *et al.*, 1975) which, in fact, solves equation (2). For this purpose we choose the following profiles of the equilibrium current and density

$$j_\theta = 0, \quad j_z = j(0)\left[1 - \left(\frac{r}{a}\right)^2\right]^{\kappa_j},$$

$$\rho = \rho(0)\left\{(1-\Delta)\left[1 - \left(\frac{r}{a}\right)^2\right]^{\kappa_\rho} + \Delta\right\}, \tag{8}$$

which represent a good parametrization of ohmically-heated Tokamaks. The exponents κ_j and κ_ρ are free parameters. In present day Tokamaks the current seems to be more peaked than the density implying that κ_j is larger than κ_ρ. The constant $j(0)$ is determined from the condition that the safety factor at the axis

$q(0) = B_z r/RB_\theta = 1$. The density at the axis $\rho(0)$ appears only in the normalizing Alfvén frequency ω_N given by

$$\omega_N^2 = \frac{B_z^2}{\rho(0)a^2\mu_0}. \tag{9}$$

The parameter Δ defines the density at the plasma boundary. If Δ equals zero, the Alfvén continuum extends to ∞. The quantity n_c can now easily be calculated

$$n_c = m\left[\frac{\kappa_j}{\kappa_\rho(1-\Delta)} - 1\right]. \tag{10}$$

We choose, as the standard case, the following values for the parameters

$$\begin{aligned} &\kappa_j = 4, \quad \kappa_\rho = 1, \\ &B_z = 1, \quad \Delta = 0.05, \\ &m = 1. \end{aligned} \tag{11}$$

These values which yield $n_c = 3.2105$.

In Fig. 2 is shown the spectrum associated with the global eigenmodes in the stable region. The distance $\Delta\omega^2/\omega_N^2$ of the eigenfrequencies from the lower edge of the Alfvén continuum is plotted as a function of n. Only the eigenfrequencies with $\Delta\omega^2/\omega_N^2 > 10^{-5}$ are given. At $n = n_c$ (marked by II) we find 13 eigenfrequencies. The number of eigenfrequencies decreases for $n < n_c$ (region I) and for $n > n_c$ (region III). For high n ($n > 7$) all the eigenfrequencies seem to disappear. For negative n numbers, the mode corresponding to the uppermost eigenfrequency becomes unstable and the other global eigenmodes disappear.

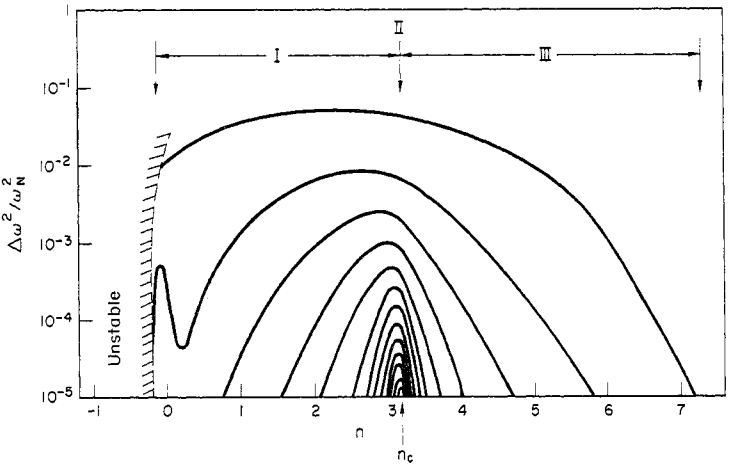

FIG. 2.—Spectrum associated with the global eigenmodes for the standard case. The distance $\Delta\omega^2/\omega_N^2$ of the eigenfrequencies from the lower edge of the Alfvén continuum is plotted vs the toroidal wavenumber n for different radial mode numbers l. For negative values of n, the mode corresponding to the uppermost eigenfrequency is unstable. In the whole range $-0.12 < n < 7.28$ there is an accumulation point at $\Delta\omega^2 = 0$. The highest density of the eigenfrequencies occurs at $n = n_c$.

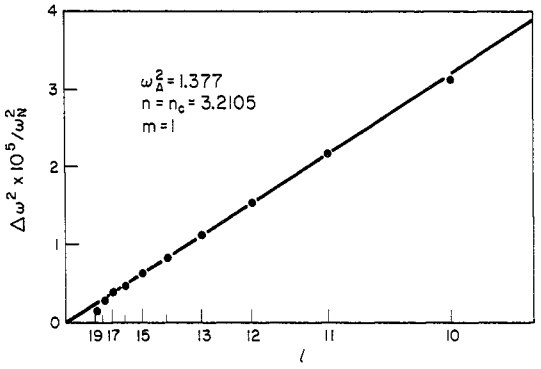

FIG. 3.—Distance $\Delta\omega^2/\omega_N^2$ at $n = n_c$ vs the radial mode number l. For $l \geq 10$, $\Delta\omega^2 \sim 1/l^4$ as predicted by the WKB analysis.

The high density of the eigenfrequencies at $n = n_c$ is demonstrated in Fig. 3. For this value of n, 19 eigenfrequencies have been found using 100 radial intervals and accumulating the mesh at the axis. The distance $\Delta\omega^2/\omega_N^2$ is plotted vs the radial mode number l. For $l > 10$ we find a $1/l^4$ dependence of $\Delta\omega^2/\omega_N^2$. In regions I and III the relative distance between the eigenfrequencies with different radial mode numbers is much larger. The spacing increases as the distance from the point $n = n_c$ increases.

The eigenmodes corresponding to three different values of n are displayed in Fig. 4. For $n = 2$ there are four radial eigenmodes in region I (Fig. 4a). These modes exhibit spatial localization around the radial position $r = r_c$ at which $d\omega_A^2/dr = 0$. In Fig. 4b the first six radial eigenmodes are shown for $n = n_c$. These modes are more localized at the axis for higher l. Even stronger localiza-

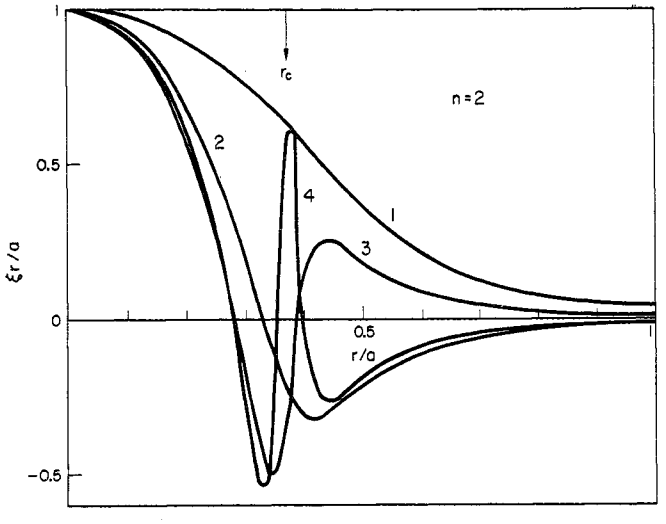

FIG. 4(a).

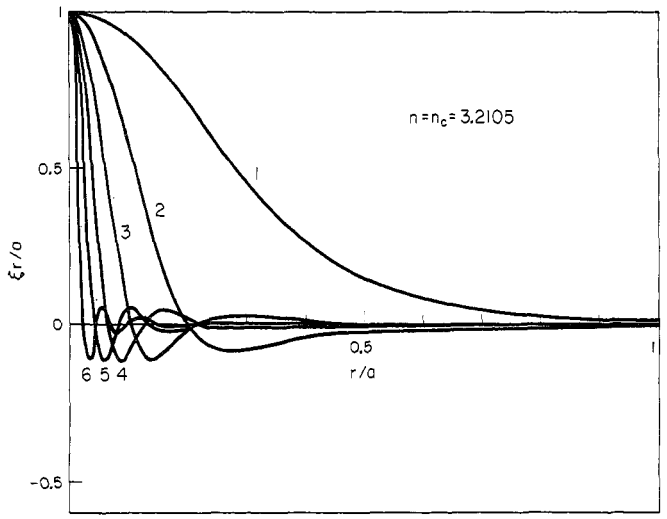

FIG. 4(b)

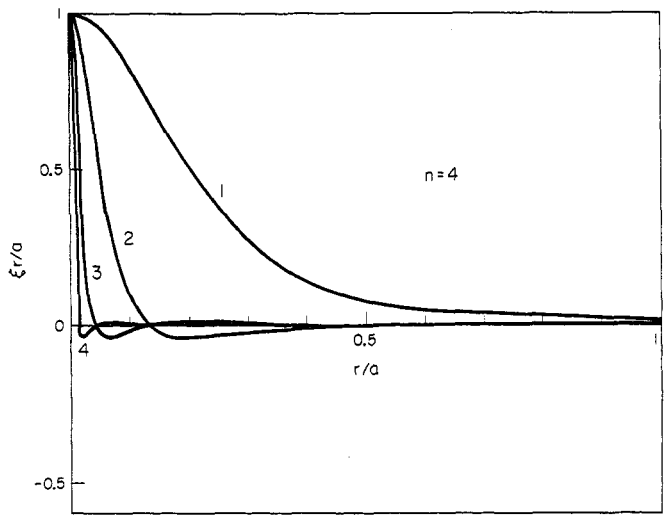

FIG. 4(c).

FIG. 4.—Radial displacement ξ_r as a function of radius for different radial mode numbers l. In 4a, the lowest four radial eigenmodes are plotted for $n = 2$ (region I); in 4b, the lowest six radial eigenmodes at the essential singularity point (II) and in 4c, the lowest four radial eigenmodes at $n = 4$ (region III) are shown. The arrow in 4a indicates the position at which $d\omega_A^2/dr = 0$.

tion at the axis is observed in Fig. 4c for the four radial eigenmodes for $n = 4$ (region III).

We shall now study these phenomena analytically.

4. ANALYTICAL INVESTIGATION OF THE GLOBAL EIGENMODES

The three regions defined above are treated separately. They are charac-

terized by

I: $$(\omega_A^2)' = 0 \quad \text{and} \quad (\omega_A^2)'' > 0 \text{ at } r = r_c \neq 0$$

II: $$(\omega_A^2)' = (\omega_A^2)'' = (\omega_A^2)''' = 0 \quad \text{and} \quad (\omega_A^2)'''' > 0 \text{ at } r = 0$$

III: $$(\omega_A^2)' = 0 \quad \text{and} \quad (\omega_A^2)'' > 0 \text{ at } r = 0.$$

Let us investigate each region:

(a) *Region* I

In this region the analytical treatment is very similar to the SUYDAM (1958) or NEWCOMB (1960) theory. The existence of global eigenmodes with eigenvalues ω^2 below the lower edge of the continuum is related to the behaviour of the solutions of the Hain–Lüst equation around $\omega^2 = \text{Min}(\omega_A^2(r))$. In particular, the edge of the continuum is an accumulation point of a discrete spectrum if the singular solution has an oscillatory singularity at $r = r_c$. To treat this case we expand $\omega^2 - \omega_A^2$ around $\text{Min}(\omega_A^2(r))$:

$$\omega^2 - \omega_A^2 \cong -\tfrac{1}{2}(\omega_A^2)''(r - r_c)^2 \equiv -\tfrac{1}{2}(\omega_A^2)'' x^2. \tag{12}$$

Equation (2) then reduces to

$$x^2 \xi_r'' + 2x\xi_r' + g_I(r_c)\xi_r = 0, \tag{13}$$

where

$$g_I = -\frac{2C}{(\omega_A^2)''}, \tag{14}$$

$$C = \frac{G^2}{\rho B^2 \mu_0}\left\{\frac{4B_\theta^4}{r^2 B^2 (1-H)^2} + r\frac{\mathrm{d}}{\mathrm{d}r}\left[\frac{B_\theta^2(1+H)}{r^2(1-H)}\right]\right\}, \tag{15}$$

$$H = \frac{FB_z}{kB^2}. \tag{16}$$

Assuming $\xi_r \sim x^\alpha$ we obtain a characteristic polynomial which indicates that oscillatory solutions are present if

$$g_I - \tfrac{1}{4} > 0. \tag{17}$$

For the standard case (see equation 11) we find

$$\begin{aligned} g_I - \tfrac{1}{4} > 0 \quad &\text{for} \quad 0 \leqslant r/a < 0.92 \quad \text{or} \quad n_c \geqslant n - 0.12, \\ g_I - \tfrac{1}{4} < 0 \quad &\text{for} \quad 0.92 < r/a \leqslant 1 \quad \text{or} \quad -0.12 > n \geqslant -0.18. \end{aligned} \tag{18}$$

This shows that there is an accumulation point in the region $-0.12 < n \leqslant n_c$ (see Fig. 2). The density of the eigenfrequencies in the vicinity of the accumulation point can be estimated by means of the same type of calculation as that used by PAO (1974) for the Suydam eigenmodes. It yields

$$\Delta\omega^2 \sim \exp[-\text{const}(g_I - \tfrac{1}{4})^{-1/2}]. \tag{19}$$

This behaviour is in accordance with the numerical results shown in Fig. 2. At $n = -0.12$, $g_I - 1/4 = 0$ and the distance between the eigenfrequencies close to the accumulation point goes to zero. In the numerical calculations, we only find two eigenfrequencies. With increasing n, $g_I - 1/4$ increases and becomes infinite at $n = n_c$, which leads to a different asymptotic behaviour. The number of eigenfrequencies also increases with increasing n in the numerical calculations.

(b) *Essential singularity* (II)

At the point $n = n_c$, the first three derivatives of ω_A^2 are equal to zero. We then have around $r = 0$

$$\omega^2 - \omega_A^2 \cong -\frac{1}{4!}(\omega_A^2)'''' r^4 \tag{20}$$

and the reduced Hain–Lüst equation reads

$$r^4 \xi_r'' + 7r^3 \xi_r' + g_{II}(r = 0)\xi_r = 0, \tag{21}$$

where

$$g_{II} = -\frac{24C}{(\omega_A^2)''''}. \tag{22}$$

By virtue of a WKB analysis we can estimate the eigenfrequencies close to the accumulation point:

$$\Delta\omega^2 \sim (\omega_A^2)'''' g_{II}^2 / l^4. \tag{23}$$

We find the same $1/l^4$ dependence as in Fig. 3.

(c) *Region* III

In this region $\omega^2 - \omega_A^2$ is again expanded around $r = 0$

$$\omega^2 - \omega_A^2 \cong -\tfrac{1}{2}(\omega_A^2)'' r^2. \tag{24}$$

The reduced Hain–Lüst equation then becomes

$$r^2 \xi_r'' + 5r\xi_r' + g_{III}(r = 0)\xi_r = 0, \tag{25}$$

where

$$g_{III} = 3 - m^2 - \frac{2C}{(\omega_A^2)''}. \tag{26}$$

Assuming $\xi_r \sim r^\alpha$ one finds a characteristic polynomial which indicates that oscillatory solutions exist if

$$g_{III} - 4 > 0. \tag{27}$$

For the standard case this criterion is satisfied in the region $n_c \leqslant n < 7.28$. The density of the eigenfrequencies in the vicinity of the accumulation point can again be estimated by means of Pao's theory giving, similar to region I (see equation 19),

$$\Delta\omega^2 \sim \exp[-\text{const}(g_{III} - 4)^{-1/2}]. \tag{28}$$

Again this behaviour is in accordance with the numerical results shown in Fig. 2. At $n = 7.28$, $g_{III} - 4 = 0$ and the distance between the eigenfrequencies close to the accumulation point tends to zero. Numerically, we cannot resolve a density of eigenfrequencies which is too high and we only see the first eigenfrequency around $n = 7$. With decreasing n, $g_{III} - 4$ increases and becomes infinite at $n = n_c$, which leads again to the asymptotic behaviour discussed earlier (essential singularity). Numerically, an increasing number of eigenfrequencies is found as $n = n_c$ is approached.

5. GLOBAL EIGENMODES IN TOROIDAL GEOMETRY

We would now like to assess to what extent plasma toroidicity affects the one-dimensional results. Unfortunately, it is not possible to use simply the two-dimensional code ERATO to detect global eigenmodes and draw a conclusion as we did in the one-dimensional case. The reason is that modes having different mode number m are now coupled through the toroidicity and, as a consequence, the continuous Alfvén spectrum extends from $\omega^2 = 0$ to $\omega^2 = \infty$. Instead, we shall consider excitation of the plasma due to an external antenna and calculate the antenna load Z as a function of the applied frequency. Any peak that appears would indicate the existence of a global eigenmode.

It is our intention to prove that toroidal effects must be considered to interpret the results of the TCA Tokamak (DE CHAMBRIER *et al.*, 1981). For this purpose we apply both a cylindrical (BALET *et al.*, 1981) and a toroidal (APPERT *et al.*, 1981) model to the equilibrium described by (11) and to the TCA parameters used by DE CHAMBRIER *et al.* (1981). In the toroidal version, the TCA antenna is best modelled by a bihelical antenna ($n = 2, m = \pm 1$). In the cylindrical version, the antenna load is obtained as a sum of the loads of two antennae with single helicity. In both cases an artificial damping ν with the value $0.003\ \omega$ is used. This value is an estimate of the electron Landau damping of the global eigenmodes for the TCA parameters.

The results obtained with the cylindrical model are shown in Fig. 5. The line-averaged density $\bar{n}$, used in Fig. 5, is directly proportional to ω^2/ω_N^2. We find a peak at $\bar{n} = 2 \times 10^{13}\ \mathrm{cm}^{-3}$ which is situated just beneath the threshold ($\bar{n}_1$) of the ($n = 2, m = 1$) Alfvén continuum. With the value of ν chosen, no other peaks (satellites) with the ($n = 2, m = 1$) helicity appear. For higher $\bar{n}$, corresponding to higher values of ω^2/ω_N^2, the antenna load increases rapidly due to the resonant absorption. No further peak appears. These two features are in disagreement with the experiment (DE CHAMBRIER *et al.*, 1981).

The results obtained with the toroidal model are shown in Fig. 6. As in the one-dimensional results (Fig. 5) a peak around $\bar{n} \lesssim \bar{n}_1$ can be seen. We find that this peak corresponds to a global eigenmode with a dominant $m = 1$ behaviour. With increasing $\bar{n}$, Z seems to increase less rapidly than in the one-dimensional case. However, numerical uncertainty due to poor radial resolution prevents us from drawing a well defined curve $Z(\bar{n})$ as in the one-dimensional case. Around $\bar{n} \lesssim \bar{n}_2$, which corresponds to the ($n = 2, m = 2$) Alfvén threshold, a second peak appears. The corresponding mode is global and dominantly $m = 2$. We therefore conclude that the ($n = 2, m = 2$) global eigenmode is observed due to the toroidal coupling. Qualitatively, the toroidal calculation is in better agreement with the experimental results than is the cylindrical calculation.

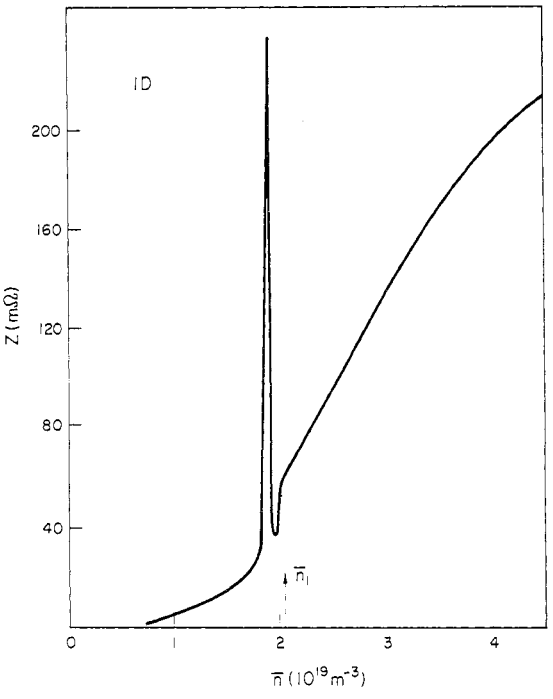

FIG. 5.—Antenna load Z vs line-averaged density as obtained using a cylindrical model. The curve was calculated for a deuterium plasma embedded in a 1.2T toroidal field with an excitation frequency of 2.67 MHz. The load of the whole antenna structure is given by 8Z. The threshold density $\bar{n}_1$ corresponds to the minimum $\bar{n}$ for which the Alfvén resonance with the helicity ($n = 2$, $m = 1$) is situated in the plasma.

6. IS "AERH" POSSIBLE?

The resonance phenomena described above could lead to a new heating scheme which we propose to call AERH (Alfvén Eigenmode Resonance Heating). The efficiency of such a heating scheme is strongly dependent on the answers to a number of questions.

First, we have to know how far the eigenfrequencies are from the continuum. The relative distance, $\Delta\omega^2/\omega_A{}^2 = 1 - \omega^2/\omega_A{}^2$, of these frequencies from the lower edge of the continuum is shown in Fig. 7 as a function of the toroidal wavenumber n. We consider the first (uppermost) and second eigenfrequencies of Fig. 2. One can see that for high n numbers ($n > 4$) the relative distance $\Delta\omega^2/\omega_A{}^2 < 1\%$ for the first radial eigenmode ($l = 1$) and $\Delta\omega^2/\omega_A{}^2 < 1‰$ for the second ($l = 2$). With decreasing n, the relative distance of the first eigenfrequency increases, reaching $\Delta\omega^2/\omega_A{}^2 = 12\%$ for $n = 1$ and 55% for $n = 0$. The second eigenfrequency develops a local minimum which disappears when the wall approaches the plasma surface. The relative distance $\Delta\omega^2/\omega_A{}^2 = 2\%$ for $n = 0$. This means that, from the practical point of view, only low-n global eigenmodes can be considered for an AERH heating scheme.

Another important consideration is the coupling to the antenna which is strongly related to the radial displacement ξ_r of the mode at the plasma surface.

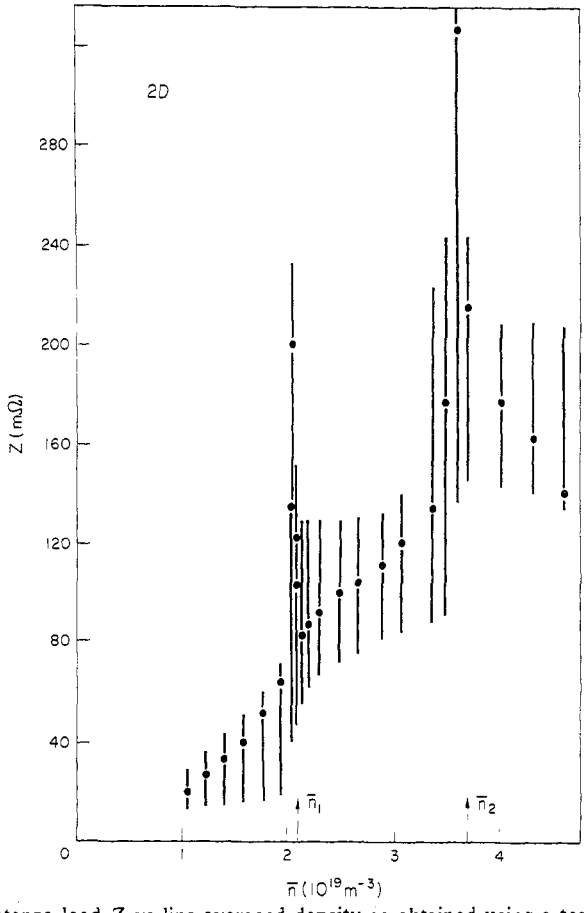

FIG. 6.—Antenna load Z vs line-averaged density as obtained using a toroidal model. The equilibrium and excitation frequency are the same as for Fig. 5. The threshold densities $\bar{n}_1$ and $\bar{n}_2$ correspond to the onset of the continua ($n = 2, m = 1$) and ($n = 2, m = 2$), respectively.

In Fig. 8 we display the behaviour of $\xi_r(r)$ corresponding to the uppermost eigenfrequency of Fig. 2 for different n numbers. We can see that this mode behaves as kink-like mode for $n = 0$ (it becomes the unstable kink for $n < 0$) and becomes more and more internal with increasing n. The arrows, which are marked for $n = 0$, 1, 2 and 3, show the radial positions in the plasma where the curve $\omega_A^2(r)$ has its minimum, i.e. where the higher radial eigenmodes concentrate (see Fig. 4). The displacement at the plasma surface, which is a measure of the coupling to the antenna, increases as n decreases. For $n = 0$ it reaches 70% of the maximal displacement.

One of the serious problems associated with r.f. heating is that often the energy is deposited close to the plasma surface. Preliminary toroidal calculations for AERH using $n > 1$ show that a large fraction of the power is deposited near the plasma surface. The situation appears to be similar to that encountered with the usual Alfvén wave heating scheme for which toroidal coupling leads to

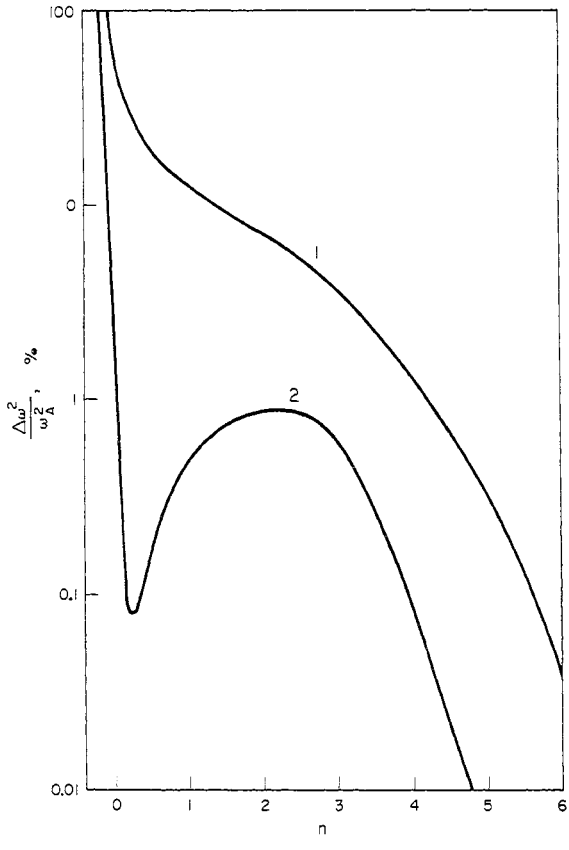

FIG. 7.—Relative distance $\Delta\omega^2/\omega_A^2$ for the first two radial eigenmodes vs n.

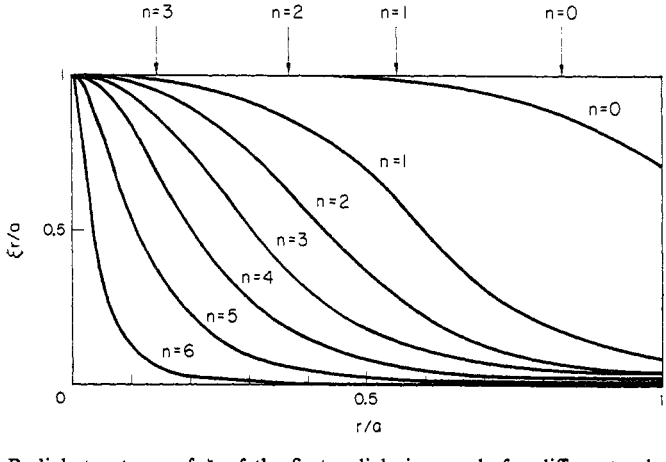

FIG. 8.—Radial structures of ξ_r of the first radial eigenmode for different values of n. The arrows indicate the radial positions where the curve $\omega_A^2(r)$ has its minimum.

surface heating (APPERT *et al.*, 1981). It therefore appears that AERH using an $n \geqslant 1$ antenna is not advantageous compared to resonant absorption. On the other hand, for the case $n = 0$, AERH has attractive features. The low frequency involved does not appear in any Alfvén continuum. Therefore, there is no possibility of coupling to the plasma surface. Since only the cases $n \geqslant 1$ can be treated with the present version of our toroidal heating code, we cannot unfortunately corroborate this assertion by a numerical calculation. Another advantageous feature of AERH is the simplicity of an $n = 0$ antenna structure. In the resonant absorption scheme the $n = 0$ antenna is not well coupled to the plasma since the global eigenmode is far from the continuum.

If AERH with the $n = 0$ antenna is to be considered, frequency tracking is certainly necessary. We know that the $n = 0$ modes are strongly affected by plasma elongation and by the position of the conducting wall. Small modifications of the plasma surface can change the resonant frequency of the $n = 0$ global eigenmode appreciably.

Acknowledgements—The authors wish to acknowledge the useful discussions with Dr. F. HOFMANN, Dr. R. KELLER, Dr. J. B. LISTER, Dr. A. POCHELON and Dr. M. L. SAWLEY. This work has been supported by the Ecole Polytechnique Fédérale de Lausanne, by the Swiss National Science Foundation and by Euratom.

REFERENCES

APPERT K., BALET B., GRUBER R., TROYON F., TSUNEMATSU T. and VACLAVIK J. (1981) Centre de Recherches en Physique des Plasmas, Lausanne, Report LRP 187/81 *Nucl. Fusion* (1982), Vol. 22,

APPERT K., BERGER D., GRUBER R., TROYON F. and ROBERTS K. V. (1975) *Comput. Phys. Commun.* **10**, 11.

APPERT K., GRUBER R. and VACLAVIK J. (1974) *Physics Fluids* **17**, 1471.

BALET B., APPERT K. and VACLAVIK J. (1982) Centre de Recherches en Physique des Plasmas, Lausanne, Report LRP 188/81, *Plasma Physics* **24**, 1005.

DE CHAMBRIER A. *et al.* (1982) Centre de Recherches en Physique des Plasmas, Lausanne, Report LRP 195/81, *Plasma Physics* **24**, 893.

HAIN K. and LÜST R. (1958) *Z. Naturforschung* **13a**, 936.

NEWCOMB W. A. (1960) *Ann. Phys.* **10**, 232.

PAO Y. P. (1974) *Nucl. Fusion* **14**, 25.

POCHELON A., KELLER R., TROYON F. and GRUBER R. (1975) *Proceedings of the 7th European Conference on Controlled Fusion and Plasma Physics*, Lausanne, Vol. I, 157.

ROSS D. W., CHEN G. L. and MAHAJAN S. M. (1982) Fusion Research Center, Austin, Texas, Report FRCR 227, *Physics Fluids* **25**, 652.

SUYDAM B. R. (1958) *Proceedings of the 2nd International Conference on the Peaceful Uses of Atomic Energy* **31**, 157.

Note added in proof:
At the Grenoble Symposium on Heating in Toroidal Plasmas A. W. Kolfschoten and T. Hellsten pointed out to us that J. P. Goedbloed was aware of the complexity of the Alfvén spectrum as early as in 1975; see *Physics Fluids* **18**, 1258 (1975).